

Selection of the model functions for calculations of high-overtone intensities in the vibrational-rotational spectra of diatomic molecules

© E.S. Medvedev, V.G. Ushakov

Institute of Problems of Chemical Physics, Russian Academy of Sciences,
142432 Chernogolovka, Moscow oblast, Russia

e-mail: medvedev@icp.ac.ru

Received May 31, 2022

Revised July 05, 2022

Accepted July 09, 2022

The initial information on the molecular functions necessary for calculations of spectra is always of discrete nature, being either quantum-chemical calculations or experimental data. Selection of the model functions built on this information and then used to calculate the intensities of the fundamental transitions and low overtones is not restricted by any conditions, yet these same functions can result in errors when used for the high-overtone transitions. In particular, the errors are found in calculations for OH, PN, YO, CaO, PS, NS, SH, PH, and NO. We analyze the sources of the errors and give recommendations of how to avoid them. The molecular functions should be chosen such that the Normal Intensity Distribution Law is fulfilled. In order to increase the accuracy of the calculations, it is also desirable that their analytical properties in the complex plane be as close as possible to those of the real functions.

Keywords: NIDL, repulsive branch, analytical functions, branch points, damped coordinate, saturation of the intensities.

DOI: 10.21883/EOS.2022.09.54822.3428-22

Introduction

The main feature of overtone transitions is a very fast decrease in intensity with increasing overtone number — the intensity drops by 1–2 orders when moving to the next overtone, so for numerical calculation of the intensities of very high overtones quadruple accuracy is required [1]. This is quantitatively described by the so-called „Normal Intensity Distribution Law“ (NIDL), according to which the logarithm of the intensity is a linear function of the square root of the upper level energy E_v in units of the vibrational quantum ω [2,3]. The exceptions are anomalies, i.e., separate lines, the intensity of which is much weaker than it follows from NIDL, due to a specific interference effect [3,4]. The normal intensity distribution law is fulfilled for all diatomic molecules, as well as for quasi-diatomic local vibrations in polyatomic molecules, which is confirmed by experimental data and theoretical calculations [2,5–7]. The physical nature of NIDL is described in detail in [3,8,9], where it is shown that it is closely related to the behavior of the molecular potential in the strong repulsion region. The normal law of intensity distribution is a powerful tool for analyzing the calculated intensities of overtone transitions.

To calculate the intensities of dipole transitions, it is necessary to know the potential energy $U(r)$ and the electric dipole moment $d(r)$ of the molecule as functions of the internuclear distance r . In the case of transitions with a small change in the vibrational quantum number v , as a rule, $\Delta v \leq 2$, the shape of these functions does not affect the result, but this is not the case for higher

overtones. In particular, using the example of calculations of the intensities of transitions $v \leftarrow 0$ for SiO, CS, CO, and LiCl, it was shown that the use of non-analytical functions with discontinuous derivatives, for example, splines, leads to nonphysical saturation of the intensities at $v \geq 5$ for SiO [10], $v \geq 7$ for CS [1,11], CO and LiCl [10]. Therefore, in modern calculations, only analytic functions are used [12], but the problem still remains, since, as we will see, additional restrictions are needed.

Further studies have shown that model functions should have special properties of analyticity in the complex plane, close to the properties of true molecular functions [13], and a method was proposed to quantify the degree of such closeness [9,13]. It is based on the obvious requirement that the results of calculations depend relatively weakly on the choice of the shape of the dipole moment function (DMF) with formally different analytical properties. See [9] for an example of similar intensities for CO calculated with an irregular DMF with branching points and with a rational function. In this case, one can expect that the remaining discrepancy gives an estimate of the accuracy of the calculation.

In this article, using NIDL, we analyze the calculation data for some diatomic molecules contained in the international databases ExoMol [14] and HITEMP [15] and propose methods for improving the calculations accuracy. Significant deviations from NIDL are interpreted as errors due to incorrect choice of DMF or potential energy function, which is justified in the Discussion. Methods for improving the calculations accuracy are considered in the Conclusion.

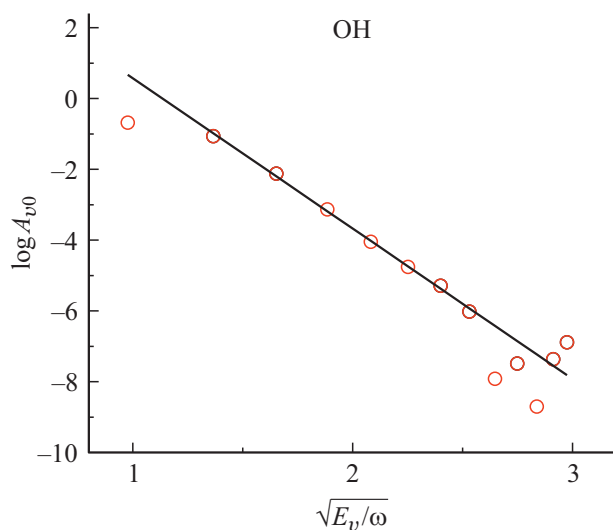


Figure 1. Calculated Einstein coefficients A_{v0} (in s^{-1}) for vibrational-rotational transitions in the ground electronic state $X^2\Pi$ of the hydroxyl radical according to [16] taken from the ExoMol database (<https://www.exomol.com/>). $J'' = 0.5$, $v = 1-13$. The NIDL straight line is drawn through the points $v = 2-8$, $\omega = 3738.465 \text{ cm}^{-1}$ [16]; point $v = 9$ — possible anomaly.

Saturation of intensities due to DMF non-analyticity

The figures below show the intensities of transitions $v', J' \leftarrow v'', J''$ from the lower state $v'' = 0, J'' = 0, 0.5, 1$ or 1.5 to the upper state $v' = v \geq 1, J' = J'' + 1$. The NIDL straight line is drawn through the points starting from the first overtone $v = 2$ excluding the anomalies.

Figure 1 shows the data by Brooke et al. [16] for the hydroxyl radical. The deviations from the NIDL linear dependence as a result of using splines occur at $v \geq 9$.

Figure 2 shows the data by Yorke et al. [17] for phosphorus nitride. The deviations from the linear dependence of NIDL due to the use of splines occur at $v \geq 6$. Wrong data at $v \geq 6$ was not included in ExoMol.

A similar situation occurs for yttrium monoxide (Fig. 3) and calcium oxide (Fig. 4). Saturation due to the use of splines was also observed for carbon monosulfide CS (Fig. 3 in [1] and Fig. 4 in [11]). In the study [11] a piecewise DMF with discontinuities of derivatives at $r = 1$ and 3.4 \AA was proposed, but this should also lead to strong deviations from NIDL.

Saturation of intensities due to rapid DMF change in the complex plane

In the study [12], taking into account our considerations about the need to use analytic functions, a model analytic DMF in the form of a polynomial in the so-called „damped“ coordinate was proposed:

$$z = (r - r_{\text{ref}}) \exp[-\beta_2(r - r_{\text{ref}})^2 - \beta_4(r - r_{\text{ref}})^4], \quad (1)$$

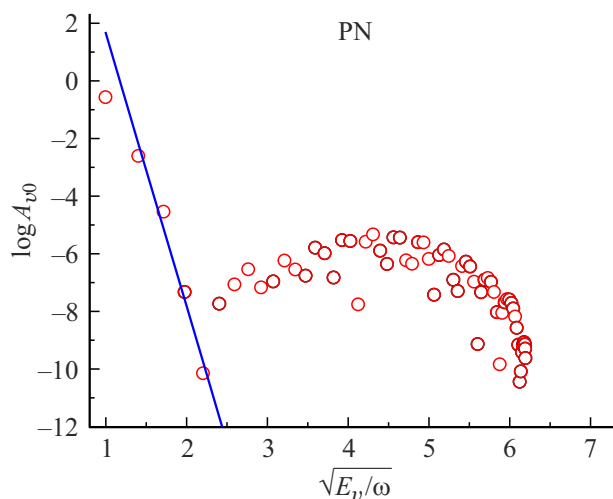


Figure 2. Einstein coefficients for transitions in the $X^1\Sigma^+$ state of phosphorus nitride according to [17]. $J'' = 0$, $v = 1-66$. The NIDL straight line is drawn through the points $v = 2-5$, the intensities at $v \geq 6$ are obviously wrong.

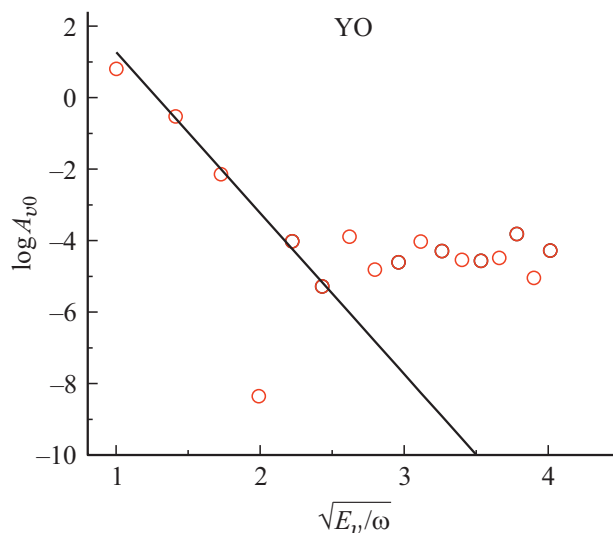


Figure 3. Einstein coefficients for transitions in the $X^2\Sigma^+$ state of yttrium monoxide according to [18]. $J'' = 0.5$. Point $v = 4$ — anomaly. The NIDL straight line is drawn through the points $v = 2, 3, 5, 6$. $\omega = 861.5 \text{ cm}^{-1}$ [18]. The intensities at $v = 7-17$ are obviously erroneous.

where r_{ref} — a fixed parameter close to the equilibrium bond length r_e , and β_2, β_4 — variable parameters. However, the polynomial in powers of the variable z does not satisfy the requirement that the DMF does not change too fast in the complex plane r [9] — DMF grows exponentially and oscillates. Unfortunately, there is no way to check whether there is a NIDL fault in at high v Fig. 5 for phosphorus monosulfide (PS), since saturation of the intensities at $v > 15$ is caused by the use of double precision in numerical calculations. Be reminded that the use of double precision in carbon monoxide CO resulted in saturation at $v > 20$ [21]

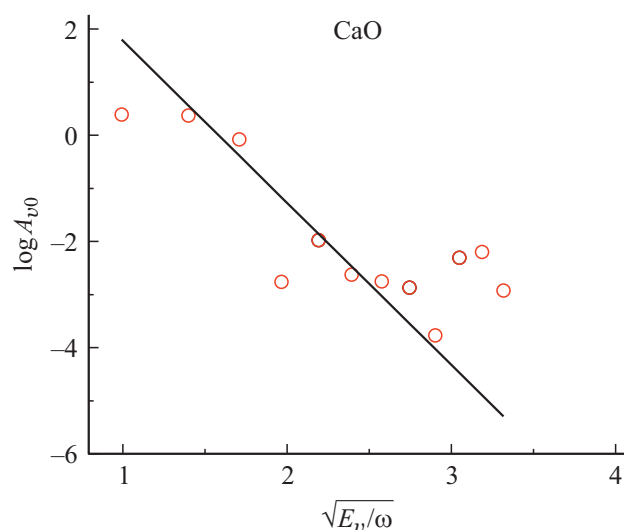


Figure 4. Einstein coefficients for transitions in the $X^1\Sigma^+$ state of calcium oxide according to [19]. $J'' = 0$. Point $v = 4$ — anomaly. The NIDL straight line is drawn through the points $v = 2, 3, 5, 6$. $\omega = 733.4 \text{ cm}^{-1}$ [20]. The intensities at $v = 7-12$ are obviously erroneous.

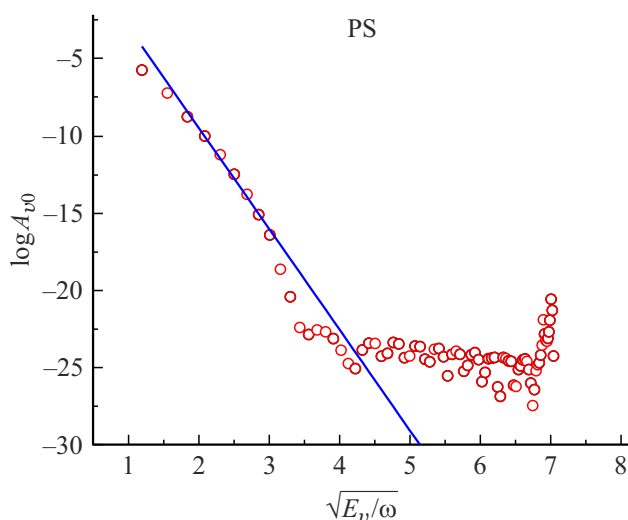


Figure 5. Einstein coefficients for transitions in the $X^2\Pi$ state of phosphorus monosulfide according to [12]. $J'' = 0.5$, $v = 1-81$. The NIDL straight line is drawn through the points $v = 2-9$. Points $v = 13$ and 19 are possible anomalies. The intensities at $v > 20$ are obviously erroneous.

with comparable values of A . A similar situation takes place for nitrogen sulfide (Fig. 6).

Let us discuss in more detail the results for thio(mercapto)-radical (Fig. 7) obtained by Yurchenko et al. [22] and Gorman et al. [23]. In the first article the transitions in an isolated ground electronic state X were considered, and in the second, excited states A and B were added along with the spin-orbital interactions $X-X$, $X-A$ and $X-B$ calculated using *ab initio* methods. Although the minimum of the A state is reached at the level of $v = 25$

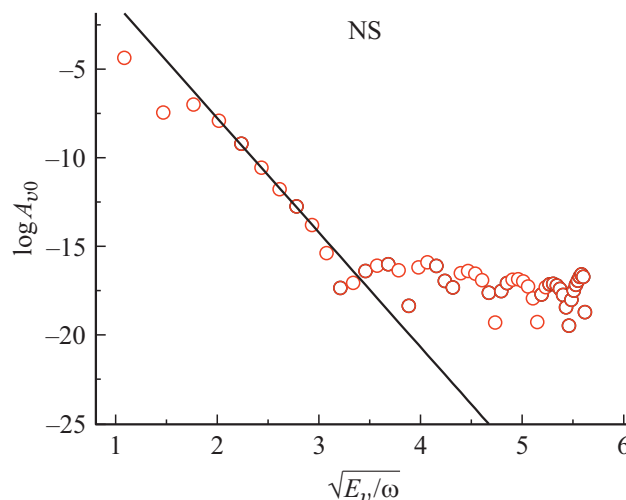


Figure 6. Einstein coefficients for transitions in the $X^2\Pi$ state of nitrogen sulfide according to [22]. $J'' = 0.5$, $v = 1-36$. NIDL straight line through points $v = 3-9$. Points $v = 2$ and 11 are possible anomalies. The intensities at $v > 12$ are obviously erroneous.

of the X state, the second article notes an appreciable contribution of the A state to the calculated absorption spectra at energies above $10\,000 \text{ cm}^{-1}$, which corresponds to level $v = 5$ of the state X . Therefore, the observed increase in intensities in the interval $v = 9-12$ could be associated with the contribution of the state A . In fact, as can be seen from the comparison of the data of these two works in Fig. 7 (circles and crosses), the contribution of the state A in the range $v = 1-14$ is relatively small and does not affect the incorrect behavior in any way, i.e. the increase in intensity above the possible anomaly at $v = 8$. As an alternative explanation for the incomprehensible growth, one can propose the influence of discontinuities in the higher DMF derivatives as a result of the use of splines for representation of the *ab initio* data or rapid changes of the DMF in the complex plane (see Discussion). We performed a simplified calculation using the Born-Oppenheimer potential (without spin-orbital interaction and small corrections) and analytical DMF, expression from [12] with parameters from [23] (dots), and the hill is gone. From this we can conclude that here splines are also to „blame“. However, in a similar situation for phosphinidene (PH), everything is different.

Data for the phosphinidene are shown in Fig. 8. The Einstein coefficients A_{v0} from the ExoMol database (circles), plotted in NIDL coordinates, behave „in waves“. For comparison, we plotted the I_{v0} overlap integral that we calculated, which exhibits an almost perfect NIDL in what follows, we use only the Born-Oppenheimer potential, ignoring the spin-orbital interaction and other contributions (the calculations showed, see pluses in Fig. 8, that this simplification has almost no effect on the results). According to the theory (appendix in [9]), the transition amplitude can be represented as the product $B_0 T_0$ of two factors. The second of these two factors depends only on the potential,

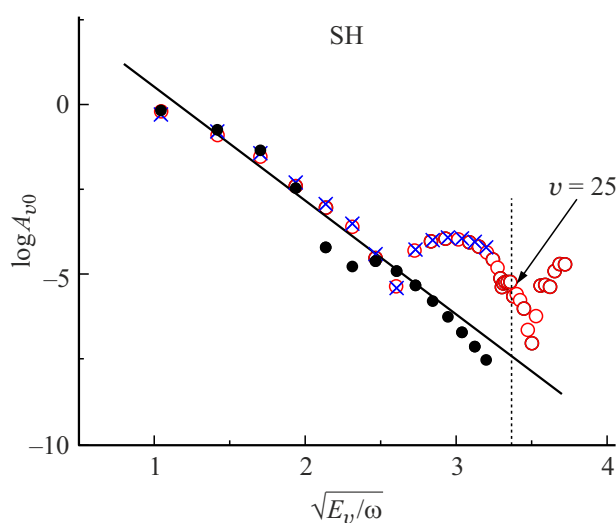


Figure 7. Einstein coefficients for transitions in the $X^2\Pi$ state of the thio(mercapto)-radical according to the data in [23] (circles, $E'' = 368 \text{ cm}^{-1}$, $v = 1-36$) and [22] (crosses, $E'' = 360 \text{ cm}^{-1}$, $v = 1-14$). Lower state: $J'' = 0.5$, $\Lambda'' = +1$, $\Sigma'' = -0.5$, $\Omega'' = +0.5$, parity e,+; upper states: $J' = 0.5$, $\Lambda' = -1$, $\Sigma' = 0.5$, $\Omega' = -0.5$, parity f,-. NIDL straight line through points $v = 2-6$, $\omega = 2711 \text{ cm}^{-1}$ [24]. Point $v = 8$ — probably anomaly. The intensities at $v > 9$ are obviously erroneous. The vertical line shows the position of the minimum of the first excited electronic state. Black circles — our calculation.

and only on its repulsive branch, and ensures a rapid decrease in intensity with the overtone number according to NIDL. The first factor, which depends on both the potential and the DMF, changes much more slowly, but can lead to „anomalies“ (i.e., weak transitions) if it passes through zero („sharp“ anomaly in the shape of a beak on a semi-log plot) or approaches zero but does not cross the x -axis („flat“ anomaly). In fact, the overlap integral is the same transition matrix element, but with $\text{DMF} \equiv 1$, so NIDL should have the same slope (same factor T_0) for any DMF, not having non-physical singularities in the complex plane and slowly changing in comparison with the wave functions of vibrational-excited states. By shifting the NIDL straight line up by a parallel translation, we see that the circles move in waves above this straight line. The reason for this behavior could be the discontinuity of the higher derivatives of the potential function at the equilibrium point r_e (see (1) in [25]), where the upper summation limit N is different to the left and right of r_e . We did the calculation with a modified potential function where $N = 1$ on both sides and got the same result shown by the squares. Therefore, DMF „is to blame“ and we have attracted our irregular function with 12 parameters [9]. First, we fit it to the analytical DMF from [25] by choosing 200 points in the interval $0-4 \text{ \AA}$ and having determined the parameter values using the least squares method, the result is shown by crosses. The amplitude of the waves has noticeably decreased, but the deviation from NIDL is still large. Then we fit it by the least squares method to 47 points *ab initio* calculated

in [25] over the interval $0.7-6 \text{ \AA}$, and the waves completely disappeared (asterisks). The failure at high transitions is explained by the non-analyticity of the potential function.

The difference in the behavior of the intensities is explained by Fig. 9, which shows how two DMFs change on the real axis and in the complex plane along a straight line parallel to the real axis. On the real axis, the two

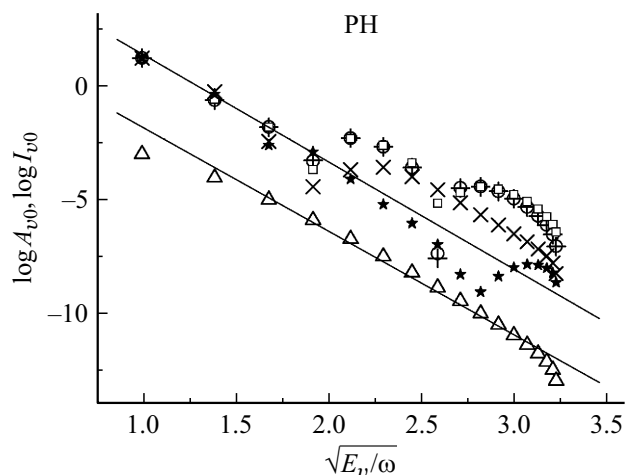


Figure 8. Einstein coefficients for transitions in the $X^3\Sigma^-$ state of phosphinidene according to [25] data (circles) and our calculations: pluses — Born-Oppenheimer potential and analytical DMF from [25]; squares — the same with modified potential (see text); crosses — potential from [25] and our irregular DMF [9] with 12 parameters fitted by the least squares method to the analytic DMF from [25]; asterisks — the same, but our DMF is fitted to *ab initio* DMF from [25]; triangles — overlap integral I_{v0} ; bottom straight line — NIDL for overlap integral; upper straight line — the same line shifted by a parallel translation; $\omega = 2365.2 \text{ cm}^{-1}$ [24]. Lower state: $E'' = 0$, $v'' = 0$, $J'' = 1$, $N'' = 0$, parity e-. Upper states $v' = 1-17$, $J' = 2$, $N' = 1$, parity e+.

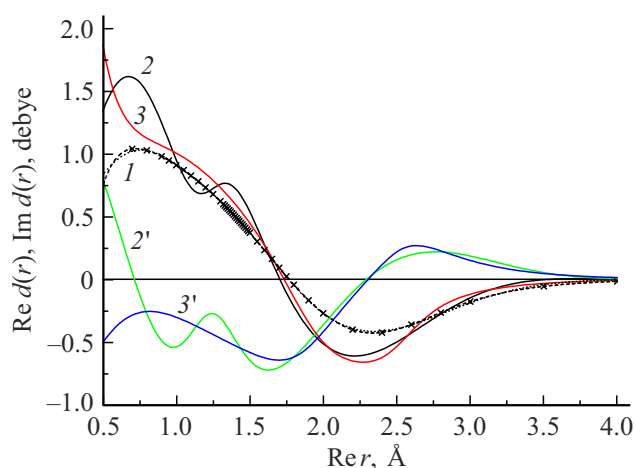


Figure 9. DMF behavior for phosphinidene (PH) on the real axis (1: crosses — *ab initio* [25], dotted line — analytical DMF from [25], dashed — our irregular DMF with 12 parameters [9]) and in the complex plane along the line $\text{Im } r = 0.4 \text{ \AA}$ (2 and 3). 2 and 2' — real and imaginary parts of DMF from [25]. 3 and 3' — the same for our irregular function.

functions are almost indistinguishable and reproduce well the *ab initio* points in the interval 1–2 Å, which makes the main contribution to the original standard integral for the transition matrix element. From this graph it is completely incomprehensible why they give such large discrepancies in intensities.

In the transformed integral (see Discussion), we shift the integration contour to the complex plane, and the main contribution comes from the region 0.7–2 Å. Along a line parallel to the real axis our irregular DMF changes smoothly, while the DMF from [25] exhibits non-physical oscillations and „winds“ around it. The latter means a very fast change of the function (large first derivative) in the region 0.7–2 Å, including $r_e = 1.422179$ Å [25], and this is reflected in the intensities of high overtones. Be reminded that NIDL was derived under the assumption that the DMF changes slowly compared to the wave functions of vibrational-excited states. As can be seen from the Fig. 8, the problems with the intensities calculated using the DMF from [25] begin at very small v .

Special case — nitric oxide

Calculations for nitric oxide (NO) were made in the studies [26–28]. The potential energy, spin-orbital interaction and dipole moment in the ground electronic state as functions of r were calculated by quantum chemistry methods in [26], then the point data were approximated by analytical and piecewise analytical functions. In particular, DMF was represented by a rational function. Although the intensity calculations were performed for all possible Δv , only $\Delta v \leq 7$ in [26] and $\Delta v \leq 16$ in [27] were included into the final line lists.

Figure 10 shows the intensities of the R(0.5) line for a very weak SR rotational band with a change in the total angular momentum projection Ω ($3/2 \leftrightarrow 1/2$), but also for strong QQ and RR bands without Ω changes ($1/2 \rightarrow 1/2$ and $3/2 \rightarrow 3/2$) the picture looks the same. The slope of the NIDL straight line a for the weak band is 4.2, and for the strong bands $a = 4.1$, the standard deviation of the points from the straight line is 0.1 in both cases. Be reminded, that the slope depends only on the steepness of the repulsive branch of the potential [3,8], it should be the same for all bands, which, as we see, is perfectly fulfilled.

Transitions up to $v = 16$ follow NIDL quite well, but for higher transitions the calculation is obviously wrong. The unusual situation is that the „wrong“ points for $v > 16$ lie below the NIDL straight line, as if there was no contribution from the repulsive branch, that should not happen (see the next section). In fact, the absolute value of the transition matrix element was limited to 10^{-9} D, that corresponds to approximately $v = 17$ according to Fig. 4 in [26], so non-zero values at $v > 16$ should really be ignored. More interesting in the mentioned Fig. 4 is the behavior of the matrix elements for $v > 16$, which were calculated without limiting their magnitude: the intensities change in waves and, obviously, they will be higher than the NIDL straight

line in the corresponding coordinates. In our Fig. 10, there is already a barely noticeable waviness in the interval $v = 7\text{--}16$, and it noticeably increases at $v > 16$ in Fig. 4 in [26]. This can be related both to the poles of the analytic functions used to approximate the potential, the spin-orbital interaction, and the dipole moment, and to the discontinuity of the higher derivatives of the potential and the spin-orbital interaction, since both the poles and the discontinuities lie near the region of classical motion.

To find out the reasons for the incorrect behavior of the intensities, we carried out an approximate calculation using only the Born-Oppenheimer potential function (without other contributions) and DMF; at the same time, we eliminated the discontinuity of the derivatives by setting the number of terms in the sum (see (2) in [26]) equal to 3 to the left and right of r_e . For $v < 17$ our calculation „by eye“ coincides with Fig. 4 of [26], but for $v > 17$ our intensities are 2–4 orders lower (not shown). As in the case of phosphinidene (PH), DMF strongly oscillates when shifted to the complex plane, which most likely explains the deviations from NIDL. It should be noted that the wrong shape of the functions cannot but affect the transitions that are low in v , hindering the achievement of the high accuracy of calculations required to solve some modern problems.

Discussion

An essential feature of overtone vibrational transitions is the extremely small value of the integral of the matrix element of the transition compared to the integrand. Note that in this case, „the exact“ calculation of the integral with the help of a computer should be treated with great care, because the calculated value can differ from the true value

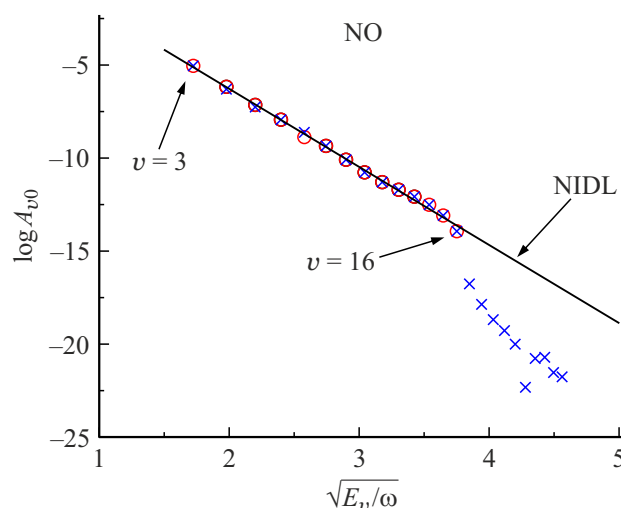


Figure 10. Einstein coefficients for nitric oxide, transitions $v' (= v)$, J' , $\Omega' \leftarrow v'' (= 0)$, J'' , Ω'' in the ground state $X^2\Pi$ of nitric oxide according to [26,27] ($v = 3\text{--}16$, circles) and [28] ($v = 3\text{--}26$, crosses). $\Omega' = J' = 1.5$, $\Omega'' = J'' = 0.5$, parity e,+; SR branch. The NIDL straight line is drawn through the points $v = 3\text{--}15$, $\omega = 1904.20$ cm $^{-1}$ [24]. The intensities at $v > 16$ are obviously erroneous.

arbitrarily and, moreover, unpredictably. Indeed, molecular functions are known only with some accuracy, but small errors in the integrand can lead to unpredictably large changes in the integral itself.

The problem with calculating this integral is that the entire domain of classical motion on the real axis contributes to it, and the integration path cannot be shifted to the complex plane, where the amplitude of the integrand could be reduced. Landau and Lifshitz [29, § 51] transformed it to another form and, shifting the integration contour C to the complex plane, showed that the main contribution to the new integral comes from the neighborhood of the singular point r_0 , where the potential function goes to infinity ($r_0 = 0$ in a diatomic molecule), i.e., not from the entire contour C , but only from the neighborhood of r_0 , where the final result is formed. It was assumed that the potential function and the DMF have no other singular points that could affect the integral value, and that the DMF slowly changes compared to the vibrational wave functions of strongly excited states. The proof included the aforementioned identical transformation of the integral, which allowed to shift the integration contour from the real axis to the complex plane and apply the steepest descent method. The goal was to reduce the integrand¹ to the value of the integral itself, that allowed to use approximate expressions for wave functions. In the original integral, as mentioned above, this was impossible, since a small change in the integrand led to an unpredictably large change in the integral.

As a result, the transition matrix element was represented as a product of the so-called „tunneling factor“, which describes the penetration of the system into the repulsion region, by a slowly varying function of ν . In the study [9] we presented it as an integral over some contour C in the complex plane, in which the maximum value of the integrand on the contour C was of the same order as the entire integral. The tunneling factor is responsible for the small value of the transition matrix element and explains the exponential decrease in the intensity with increasing transition energy [9], i.e. NIDL (see below) and its relation to the repulsive branch of the potential function. The term „tunneling factor“ implies its interpretation as the amplitude of tunneling from the left turning point in the lower state towards r_0 , followed by a transition to the upper state at some point belonging to the neighborhood r_0 , and „reverse tunneling“ to the left turning point of the upper state. A similar phenomenon is known in the theory of collisions and nonradiative transitions as „dynamic tunneling“ [30].

The molecule potential and dipole moment are formed due to the electrostatic interaction of charges, which is described by the Coulomb function $1/r$. As mentioned above, the potential function has a singular point $r_0 = 0$, where it tends to infinity due to internuclear repulsion. However, there are other singular points associated with the electronic contribution to the energy, namely branch

points [29, §79] at intersections of electronic terms for complex values of r . DMF also has branches at the same points [13]. We have shown that the pole of the potential at zero, or more precisely, the presence of a repulsive branch leads to NIDL [3] and that the branches do not distort NIDL [13]. Thus, the analytic properties of real molecular functions results in that the intensities of overtone transitions follow NIDL, and, obviously, the corresponding model functions should also obey this rule.

The Coulomb function decreases not only on the real axis, but also in any direction in the complex plane. Therefore, the model functions, at least, should not increase rapidly in the complex plane. Our calculations for CO show that a moderate power-law increase of DMF (with a power of 8 [9]) does not distort NIDL. If the DMF oscillates or grows exponentially, as in (1), then the linear dependence of NIDL is distorted, as shown in the figures. It is important to emphasize that we are talking about fast changes in the DMF precisely in the complex plane, where the main contribution to the transformed integral is formed, while there may not be fast changes on the real axis, as shown in Fig. 9 for the PH. A rapid increase in the model functions prevents the contour from shifting to the upper half-plane, which reduces the absolute value of the integrand to the value of the integral itself (see the beginning of this section). As a result, the value of the integral is no longer determined by the point r_0 , but by another area, which leads to an increase in the calculation error.

Deviations from NIDL are unacceptable, because they mean a very strong, several times and orders of magnitude, change in intensities (the division price on our graphs is 5 orders of magnitude!), which makes the calculation meaningless. We emphasize once again that the „straight“ NIDL has a deep physical basis: it is associated with the repulsive branch of the molecular potential, while deviations from NIDL are caused by specific analytical properties of the DMF and the potential, which are properties of a specific model, and not of a real molecule, and vary greatly as the model changes. The general requirement is that it is necessary to consider only those models that give the straight NIDL, then the remaining relatively small discrepancies can be treated as calculation errors. For further refinement of the model, one can use anomalies that are very sensitive to the choice of functions [31].

Note that the mentioned deviations from NIDL, caused by non-physical features of the potential and dipole moment, should always lead to an increase in intensities, because in the presence of several singular points, the integral is determined by the one that gives the maximum contribution [29]. From this point of view, the result for NO in Fig. 10 is noteworthy, where the intensities of high transitions are lower than those expected according to NIDL. This behavior clearly indicates the presence of a technical error.

It is important to emphasize that specific requirements for model functions, such as limited growth or no oscillations in the complex plane, may not be met, unless this leads to distortion of NIDL; nevertheless, in this case, too, one

¹ integrand multiplied by the width of the integration region, which is by the order of 1 Å

can expect an increase in the calculation error of not only high, but also low overtones. In particular, the presence of nonphysical poles on the imaginary axis of the potential of Meshkov et al. [32] for CO, although it does not distort NIDL, can introduce an additional error in the intensity of all lines, so that in the future it is desirable to construct a potential without such features. The use of the Šurkus variable in the model functions of the potential and dipole moment [22] can also cause deviations from NIDL due to the presence of poles in it.

We should also pay attention to the fruitfulness of using several DMFs with significantly different analytical properties to compare the results of calculating the rotational intensity distributions in vibrational bands, as we demonstrated for the 7–0 band of the CO [9,13] molecule. These can be the functions which are completely regular in any finite part of the complex plane, for example, polynomials; functions with poles, such as Padé approximants and other rational functions; branching functions. If it turns out that the distributions are very different [13], this indicates a defect in one of them or all functions. If, on the contrary, the distributions are very similar [9], then all functions are correct and the remaining difference can be treated as a calculation error.

Conclusion

A modern approach to the formation of spectroscopic databases, such as HITRAN [33], HITEMP [15], ExoMol [14,34], etc., is to include in them all possible, even very weak transitions. Special programs [35,36] have been developed for calculating the frequencies and intensities of vibrational-rotational transitions in diatomic molecules using model molecular functions which parameters are chosen on the basis of experimental and theoretical data. Recently more and more attention has been paid to the problem of increasing the accuracy of calculations, which promises new applications [35]. However, this problem is considered only in terms of the accuracy of the numerical solution of the Schrödinger equation for given functions of potential energy, dipole moment, etc., while the choice of the shape of functions often remains outside the scope of these studies.

To obtain reliable predictions of the intensities of overtone vibrational-rotational transitions it is necessary to choose such model functions which provide „straight“ NIDL (except for isolated anomalies) in a wide transition region up to the limit of dissociation. Very high transitions in themselves are of no practical interest due to the impossibility of observing them, however, they serve as an indicator, a sort of „magnifying glass“, which makes it possible to see defects in the model functions, which lead to a significant increase in the calculation error for all transitions, including low overtones.

To improve the accuracy of calculations, it is also desirable that, in terms of their analytical properties, the model functions should be as close as possible to the real functions. In particular, the model potential may

have a pole which creates a repulsive branch, and may also have branches which imitate the intersection points of electronic terms in the complex plane; at the same points, the dipole moment should have branches too [13]. The popular generalized Morse functions using the Šurkus variable, strictly speaking, do not meet these criteria due to the presence of non-physical poles. The potential of Meshkov et al. [32] for CO has a physical pole at zero, but its other poles have no physical meaning. We emphasize that the requirement formulated here regarding the analytical properties of functions is not strict — only the requirement of NIDL „straightness“ is strict. For example, the Morse potential does not have a pole at zero, and yet the presence of a repulsive branch is already enough for the NIDL to be „straight“ with a proper choice of DMF; the potential of Meshkov and co-authors, as mentioned above, has non-physical poles, which, however, do not spoil the NIDL.

Attention should also be paid to the DMF behavior when shifted to the complex plane: if the DMF oscillates, as we saw in PH and NO, this can be an obstacle to achieving the high accuracy required for some promising applications [35].

About analytical properties — the presence of common branch points, the absence of non-physical poles of the potential and dipole moment, the correct asymptotic behavior at zero and at infinity, etc. — one can say this: the closer they are to the properties of real functions, the smaller the error in calculating not only high, but also low overtones. However, the practical implementation of this strategy requires a lot of work.

Acknowledgements

The authors are grateful to R. Hargreaves and Q. Qu for the data files for Fig. 10 and to S.N. Yurchenko for the help in working with the ExoMol and HITEMP databases and helpful discussions.

Funding

The study was carried out in accordance with the state order, state registration number AAAA-A19-119071190017-7.

Conflict of interest

The authors declare that they have no conflict of interest.

References

- [1] E.S. Medvedev, V.V. Meshkov, A.V. Stolyarov, I.E. Gordon. *J. Chem. Phys.*, **143**(16), 154301 (2015). DOI: 10.1063/1.4933136
- [2] E.S. Medvedev. *Opt. Spectrosc.*, **58**(6), 741 (1985).
- [3] E.S. Medvedev. *J. Chem. Phys.*, **137**(17), 174307 (2012). DOI: 10.1063/1.4761930
- [4] E.S. Medvedev. *Sov. J. Chem. Phys.*, **5**(2), 248–257 (1989).
- [5] E.S. Medvedev. Determination of a new molecular constant for diatomic systems. Normal intensity distribution law for overtone spectra of diatomic and polyatomic molecules

- and anomalies in overtone absorption spectra of diatomic molecules. Chernogolovka: Institute of Chemical Physics, USSR Academy of Sciences, 1984. 48 pp. DOI: 10.5281/zenodo.11918.
- [6] E.S. Medvedev. *Sov. Phys.-Dokl.*, **30** (10), 853–854 (1985).
 - [7] E.S. Medvedev. *Sov. J. Chem. Phys.*, **4** (12), 2664–2670 (1989).
 - [8] E.S. Medvedev, V.I. Osherov. *Radiationless Transitions in Polyatomic Molecules*. Springer Series in Chemical Physics, ed. by V.I. Goldanskii, F.P. Schäfer, and J.P. Toennis, Vol. 57 (Springer-Verlag, Berlin, 1995). 374 pp. DOI: 10.13140/2.1.4694.7845.
 - [9] E.S. Medvedev, V.G. Ushakov. *J. Quant. Spectrosc. Radiat. Transfer*, **288**, 108255 (2022). DOI: 10.1016/j.jqsrt.2022.108255
 - [10] E.S. Medvedev, V.V. Meshkov, A.V. Stolyarov, V.G. Ushakov, I.E. Gordon. *J. Mol. Spectrosc.* **330**, 36–42 (2016). DOI: 10.1016/j.jms.2016.06.013
 - [11] S. Hou, Z. Wei. *Astrophys. J. Suppl. Ser.* **246** (1), 14 (2020). DOI: 10.3847/1538-4365/ab61ef
 - [12] L. Prajapat, P. Jagoda, L. Lodi, M.N. Gorman, S.N. Yurchenko, J. Tennyson. *Mon. Not. R. Astron. Soc.*, **472**, 3648–3658 (2017). DOI: 10.1093/mnras/stx2229
 - [13] E.S. Medvedev, V.G. Ushakov. *J. Quant. Spectrosc. Rad. Transfer*, **272**, 107803 (2021). DOI: 10.1016/j.jqsrt.2021.107803
 - [14] J. Tennyson, S.N. Yurchenko. *Int. J. Quant. Chem.*, **117**, 92–103 (2016). DOI: 10.1002/qua.25190
 - [15] L.S. Rothman, I.E. Gordon, R.J. Barber, H. Dothe, R.R. Gamache, A. Goldman, V.I. Perevalov, S.A. Tashkun, J. Tennyson. *J. Quant. Spectrosc. Radiat. Transfer*, **111** (15), 2139–2150 (2010). DOI: 10.1016/j.jqsrt.2010.05.001
 - [16] J.S.A. Brooke, P.F. Bernath, C.M. Western, C. Sneden, M. Afşar, G. Li, I.E. Gordon. *J. Quant. Spectrosc. Radiat. Transfer*, **168**, 142–157 (2016). DOI: 10.1016/j.jqsrt.2015.07.021
 - [17] L. Yorke, S.N. Yurchenko, L. Lodi, J. Tennyson. *Mon. Not. R. Astron. Soc.*, **445**, 1383–1391 (2014). DOI: 10.1093/mnras/stu1854
 - [18] A.N. Smirnov, V.G. Solomonik, S.N. Yurchenko, J. Tennyson. *Phys. Chem. Chem. Phys.*, **21**, 22794–22810 (2019). DOI: 10.1039/c9cp03208h
 - [19] S.N. Yurchenko, A. Blissett, U. Asari, M. Vasilios, C. Hill, J. Tennyson. *Mon. Not. R. Astron. Soc.*, **456**, 4524–4532 (2016). DOI: 10.1093/mnras/stv2858
 - [20] A.A. Radzig, B.M. Smirnov. *Reference Data on Atoms, Molecules, and Ions*. Springer Series in Chemical Physics, ed. by V.I. Goldanskii, F.P. Schäfer, and J.P. Toennies. Vol. 31 (Springer, Berlin, 1985).
 - [21] V.V. Meshkov, A.Yu. Ermilov, A.V. Stolyarov, E.S. Medvedev, V.G. Ushakov, I.E. Gordon. *J. Quant. Spectrosc. Rad. Transfer*, **280**, 108090 (2022). DOI: 10.1016/j.jqsrt.2022.108090
 - [22] S.N. Yurchenko, W. Bond, M.N. Gorman, L. Lodi, L.K. McKemmish, W. Nunn, R. Shah, J. Tennyson. *Mon. Not. R. Astron. Soc.*, **478** (1), 270–282 (2018). DOI: 10.1093/mnras/sty939
 - [23] M.N. Gorman, S.N. Yurchenko, J. Tennyson. *Mon. Not. R. Astron. Soc.*, **490**, 1652–1665 (2019). DOI: 10.1093/mnras/stz2517
 - [24] K.P. Huber, G. Herzberg. *Molecular Spectra and Molecular Structure. IV. Constants of Diatomic Molecules* (Van Nostrand, New York, 1979).
 - [25] J. Langleben, J. Tennyson, S.N. Yurchenko, P. Bernath. *Mon. Not. R. Astron. Soc.*, **488**, 2332–2342 (2019). DOI: 10.1093/mnras/stz1856
 - [26] A. Wong, S.N. Yurchenko, P. Bernath, H.S.P. Müller, S. McConkey, J. Tennyson. *Mon. Not. R. Astron. Soc.*, **470**, 882–897 (2017). DOI: 10.1093/mnras/stx1211
 - [27] R.J. Hargreaves, I.E. Gordon, L.R. Rothman, S.A. Tashkun, V.I. Perevalov, A.A. Lukashevskaya, S.N. Yurchenko, J. Tennyson, H.S.P. Müller. *J. Quant. Spectrosc. Rad. Transfer*, **232**, 35–53 (2019). DOI: 10.1016/j.jqsrt.2019.04.040
 - [28] Q. Qu, S.N. Yurchenko, J. Tennyson. *Mon. Not. R. Astron. Soc.*, **504** (4), 5768–5777 (2021). DOI: 10.1093/mnras/stab1154
 - [29] L.D. Landau, E.M. Lifshitz. *Quantum Mechanics: Non-Relativistic Theory*. 3rd ed. (Pergamon, Oxford, 1977).
 - [30] E.J. Heller, R.C. Brown. *J. Chem. Phys.*, **79** (7), 3336–3351 (1983). DOI: 10.1063/1.446235
 - [31] E.S. Medvedev, V.G. Ushakov. *J. Mol. Spectrosc.*, **349**, 60–64 (2018). DOI: 10.1016/j.jms.2018.04.008
 - [32] V.V. Meshkov, A.V. Stolyarov, A.Yu. Ermilov, E.S. Medvedev, V.G. Ushakov, I.E. Gordon. *J. Quant. Spectrosc. Rad. Transfer*, **217**, 262–273 (2018). DOI: 10.1016/j.jqsrt.2018.06.001
 - [33] I.E. Gordon, L.S. Rothman, R.J. Hargreaves, R. Hashemi, E.V. Karlovets, F.M. Skinner, E.K. Conway, C. Hill, R.V. Kochanov, Y. Tan, P. Wcisło, A.A. Finenko, K. Nelson, P.F. Bernath, M. Birk, V. Boudon, A. Campargue, K.V. Chance, A. Coustenis, B.J. Drouin, J.M. Flaud, R.R. Gamache, J.T. Hodges, D. Jacquemart, E.J. Mlawer, A.V. Nikitin, V.I. Perevalov, M. Rotger, J. Tennyson, G.C. Toon, H. Tran, V.G. Tyuterev, E.M. Adkins, A. Baker, A. Barbe, E. Cané, A.G. Császár, A. Dudaryonok, O. Egorov, A.J. Fleisher, H. Fleurbaey, A. Foltynowicz, T. Furtenbacher, J.J. Harrison, J.M. Hartmann, V.M. Horneman, X. Huang, T. Karman, J. Karns, S. Kassi, I. Kleiner, V. Kofman, F. Kwabia-Tchana, N.N. Lavrentieva, T.J. Lee, D.A. Long, A.A. Lukashevskaya, O.M. Lyulin, V.Y. Makhnev, W. Matt, S.T. Massie, M. Melosso, S.N. Mikhailenko, D. Mondelain, H.S.P. Müller, O.V. Naumenko, A. Perrin, O.L. Polyansky, E. Raddaoui, P.L. Raston, Z.D. Reed, M. Rey, C. Richard, R. Tóbiás, I. Sadiek, D.W. Schwenke, E. Starikova, K. Sung, F. Tamassia, S.A. Tashkun, J.V. Auwera, I.A. Vasilenko, A.A. Vigasin, G.L. Villanueva, B. Vispoel, G. Wagner, A. Yachmenev, S.N. Yurchenko. *J. Quant. Spectrosc. Rad. Transfer*, **277**, 107949 (2022). DOI: 10.1016/j.jqsrt.2021.107949
 - [34] J. Tennyson, S.N. Yurchenko, A.F. Al-Refaie, V.H.J. Clark, K.L. Chubb, E. Conway, A. Dewan, M.N. Gorman, C. Hill, A.E. Lynas-Gray, T. Mellor, L.K. McKemmish, A. Owens, O. Polyansky, M. Semenov, W. Somogyi, G. Tinetti, A. Upadhyay, I. Waldmann, Y. Wang, S. Wright, O.P. Yurchenko. *J. Quant. Spectrosc. Rad. Transfer*, **255**, 107228 (2020). DOI: 10.1016/j.jqsrt.2020.107228
 - [35] I.I. Mizus, L. Lodi, J. Tennyson, N.F. Zobov, O.L. Polyansky. *J. Mol. Spectrosc.*, **386** (4), 111621 (2022). DOI: 10.1016/j.jms.2022.111621
 - [36] S.N. Yurchenko, L. Lodi, J. Tennyson, A.V. Stolyarov. *Comp. Phys. Commun.*, **202**, 262–275 (2016). DOI: 10.1016/j.cpc.2015.12.021